International Journal of Biological Macromolecules 107 (2018) 2298–2311

Contents lists available at ScienceDirect

International Journal of Biological Macromolecules

journal homepage: www.elsevier.com/locate/ijbiomac

Antimicrobial, antioxidant and anticancer activities of zinc nanoparticles prepared by natural polysaccharides and gamma radiation

Ahmed I. El-Batal[a,*], Farag M. Mosalam[a], M.M. Ghorab[b], Amro Hanora[c], Ahmed M. Elbarbary[d]

[a] Drug Radiation Research Department, Biotechnology Division, National Center for Radiation Research and Technology (NCRRT), Atomic Energy Authority, Egypt
[b] Pharmaceutical Department, Faculty of Pharmacy, Suez Canal University, Egypt
[c] Microbiology and Immunology Department, Faculty of Pharmacy, Suez Canal University, Egypt
[d] Radiation Research of Polymer Chemistry Dept., National Center for Radiation Research and Technology, Atomic Energy Authority, Cairo, Egypt

ARTICLE INFO

Article history:
Received 23 August 2017
Received in revised form 9 October 2017
Accepted 17 October 2017
Available online 31 October 2017

Keywords:
Radiation
ZnNPs
Pectin
Chitosan
Cytotoxicity
Antimicrobial activity

ABSTRACT

Aqueous dispersed zinc nanoparticles (ZnNPs) were synthesized using natural polysaccherides (chitosan (CS), citrus pectin (CP) and alginate (Alg)) using aqueous fermented fenugreek powder (FFP) by *Pleurotus ostreatus* as reducing and stabilizing agent or using gamma irradiation. The synthesized ZnNPs are characterized by ultra violect spectroscopy (UV), Transmission electronmicroscopy (TEM), Dynamic light scattering (DLS), X-ray diffraction (XRD), and Fourier transform infrared spectroscopy (FT-IR). XRD analysis of the ZnNPS confirmed the formation of metallic nanoparticles. The nucleation and growth mechanism of ZnNPs is also discussed. TEM showed that the average diameter of ZnNPs was in the range of 46 nm. The size of nanoparticles is influenced by certain parameters such as the choice of stabilizer, pH during synthesis and absorbed dose. Evaluating the antioxidant and anticancer activities of ZnNPs was performed. The results indicating the ZnNPs synthesized by aqueous fermented fenugreek extract have high activity and the average size is 46 nm. The results explored that ZnNPs show anticancer activity against Ehrlich Ascites Carcinoma (EAC) and human colon adenocarcinoma (CACO) and the $IC_{50\%}$ was 47.5 μg/ml and 65 μg/ml respectively. Also, ZnNPs had excellent bactericidal activity against gram positive and negative bacteria and yeast.

1. Introduction

Nanotechnology possesses the potential to impact many aspects of food and agricultural systems. Food security, disease treatment delivery methods, new devices for molecular and cellular biology, new substances for pathogen detection and protection of the situation are examples of the major links of nanotechnology to the science and engineering of agriculture and food systems [1]. The efficient carrier properties of nanopartilcles have improved their use in cancer treatment. The NPs can be employed to treat cancer by either passive or active process. A passive process takes advantage of the enhanced permeability and maintenance effect. The leaky vasculature found in cancerous tissue enables NPs to diffuse easily into the cancerous tissue and kill cells [2].

Synthesis and modification of metal nanoparticles is dependent on their size, shape and distribution for developing the technology of nano-materials fields. The metallic nanoparticles such as gold, silver, iron, zinc and metal oxide nanoparticles showed interesting in biomedical applications [3–6]. Zinc oxide is unique material that exhibits semiconducting, piezoelectric, and pyroelectric properties and has varied applications in transparent electronics, ultraviolet (UV) light matters, piezoelectric devices, chemical sensors, spin electronics, personal care products, coating and paints [7].

Zinc oxide particles can be develop by several techniques such as chemical precipitation, spray pyrolysis, sol–gel, thermal decomposition, and hydrothermal synthesis electrochemical, biological and photochemical reduction techniques [8]. Increasing awareness

* Corresponding author.
E-mail addresses: aelbatal2000@gmail.com, ahmed.elbatal@eaea.org.eg (A.I. El-Batal).

https://doi.org/10.1016/j.ijbiomac.2017.10.121
0141-8130/

towards green chemistry has led to the development to fan eco-friendly approach for the synthesis of metal oxide nanoparticles. Plants, their extracts andnatural polysaccharides afford a natural synthesis route of several metallic nanoparticles, which are more eco-friendly and provides a controlled synthesis with well-defined size and shape; the enzymes, leaf extract, and bacteria play a vital role in the biological synthesis of zinc oxide nanoparticles [9].

Recently, there is a growing need to develop environmentally friendly nanoparticle synthesis methods which de not use toxic materials in the synthesis procedures. Biological processes for nanoparticle synthesis using microorganisms, enzymes, plants, and algae have been proposed as feasible eco-friendly alternatives to chemical and physical techniques because they are hazardous and costly [10]. More recently, use of eco-friendly benign materials similar leaf extract, bacteria, and fungus for the preparation of ZnNPs offers numerous advantages of Eco friend lines and compatibility for pharmaceutical and other biomedical applications [11–13], where toxic materials remain not used for the synthesis producers. Both unicellular and multicellular organisms have been employed to produce intracellular or extracellular inorganic nanomaterial's [14]. Most fungi are chosen instead of bacteria because of their tolerance and better metal bioaccumulation ability [15].

Indiscriminate use of antibiotics has reached to the biogenesis of mutant strains of microorganisms that are resistant to antibiotics and antimicrobial medicines. Zinc is a vital element, levels above threshold level inhibits bacterial enzymes such as glutathione reductase, thiol peroxidase, dehydrogenase acting as an antibacterial agent [16–18].

The present study describes green chemical (natural polysaccharides) and biological (fermented fenugreek) processes for synthesis and characterization of Zn nanoparticles. Natural polysaccharide such as CS or Alg can form various biochemical linkages with metals components, thus improving the establishment of the nano molecules. Polysaccharides have low toxicity, safe for antioxidants, antimicrobial, anticancer applications [19,20]. Fenugreek: Scientific Name: Trigonella foenum-graecum L. Family: Fabaceae (beans) these composites are glycosides of diosgenin seeds contain 0.1% to 0.9% diosgenin Many coumarin compounds known in fenugreek seeds as well as some alkaloids (e.g., trigonelline, gentianine, carpaine) [21]. It is found that the extracts of living organisms act as reducing and as capping agents in the synthesizing process of the nanoparticles [22]. Solid state fermentation (SSF) of a safe plant matrix by filamentous fungi is a biotechnological approach that may induce health profitable naturally occurring antioxidant components, including polyphenols during microbial fermentation [23].

Gamma radiation has been proved to act as an uncomplicated and efficient method for metals nanoparticles synthesis, needs an aqueous system, room temperature and ambient pressure [24,25]. The hydrated electrons produced during γ-irradiation can reduce metal ions to metal particles of zero valences [26,27], without use of reducing agents. Furthermore, the amount of zero-valent nuclei can be controlled by varying the absorbed dose of the irradiation is favourable to result highly dispersed nanoparticles. Also, the gamma radiation method which is a promising technique to fabricate a wide scale of different polymeric materials [28–32].

In this study, ZnNPs was synthesized by Natural Polysaccharidesusing using extract of fermented fenugreek and Gamma radiation and characterized by different techniques including chemical process using natural polysaccharide such as (CP, CS and Alg) and biological process employing aqueous extract of fermented fenugreek by Pleurotus ostreatus (AEFF) using gamma irradiation. The antimicrobial, antioxidant and anticancer activities of zinc nanoparticles had been estimated.

2. Experimental

2.1. Materials and methods

Citrus pectin powder (CP), chitosan (CS), sodium alginate (Alg), zinc nitrate and were obtained from Sigma-Aldrich Chemie, GmbH (Germany). Other reagents and solvents were of analytical grade.

2.2. Preparation of zinc nanoparticle (ZnNPs)

2.2.1. Using natural polysaccharides and gamma radiation

ZnNPs were synthesized using three different natural polysaccharides (CP, Alg, and CS) as follows: homogeneous solution of CS solution (1% w/v was dissolved in dilute acetic acid solution 1% w/v) or Alg (1% w/v was dissolved in deionized water) or CP, (1% w/v was dissolved in deionized water) was prepared at 60 °C while stirring overnight. The prepared solutions were filtered to remove any impurities or undissolved polymer. Then, zinc nitrate (2 mM) solution mixed with the prepared polymer solution with the ration (1:1 v/v). The solution mixtures containing zinc nitrate were stirred at room temperature and the pH was kept at pH 7 then exposed to gamma rays at different doses of 0, 10, 20, 40, 60, 80, and 100 kGy (dose rate of 2.05 kGy/h). Then ZnNPs were immediately characterized by UV–vis spectroscopy.

2.2.2. Using aqueous extract of fermented fenugreek

Aqueous extract of fermented fenugreek prepared as follows: Fungal strain; locally isolated fungal strain: *Pleurotus ostreatus* used in the study obtained from the culture stock in the Pharmaceutical Microbiology Laboratory, Drug Radiation Research Department (NCRRT, Egypt). The Strain was microscopically identified and kept on potato dextrose agar (PDA) at 4 °C and periodically sub-cultured to maintain viability.

Fermentation medium (solid state); Fermentation done in 250 ml Erlenmeyerflasks, where 15 ml of distilled water were added to 10gm fenugreek seed and powder (60% moisture content) individual and autoclaved at 121 °C for 20 min. The fungal added to the medium as a 2 ml spore suspension (8×10^6 spores/ml) and incubated at 30 °C statically in complete darkness for 10days. After ten days, full contents of the flasks (inoculated and uninoculated) were macerated in deionized water (1gm/10 ml) and seated in a shaker at 200 rpm (LAB-Line R Orbit Environ, U.S.A) for 2.0 h.

Then centrifuged (cooling centrifugeHettich Universal 16 R, Germany) for 10 min at 5 °C; the supernatant was divided from the sediment and used for an experiment.

Zinc nitrate 1 mM solution mixe with aqueous extract of fermented fenugreek (seed: powder) and unfermented (seed: powder) (1:1 v/v). The mixture stirred at room temperature and exposed to gamma ray at 0, 10, 20, 30, 40, 50 and 60 kGy. Then ZnNPs were immediately characterized by UV–vis.

2.3. Experimental factorial design

Used to compare the effect of heat and radiation on the synthesis of ZnNPs by an aqueous extract of fermented fenugreek powder. Certain factors chose as they were considered to have the most significant effect on the ZnNPs production. The levels selected based on knowledge acquired from initial experimental trials. The statistical software package (Minitab 16, U.S.A) used for designing the test, regression, analysis of experimental data and in plotting the relationship between variables.

Effect of temperature; the influences of the three variables in two level, the pH of the reaction mixture (4, 7, and 10), the concentration of zinc ions (0.1 mM, 1 mM, and 2 mM), and temperature of

the reaction mixture (20 °C, 60 °C, and 100 °C). The effect of radiation; the influence of the two variables in two level: concentration of zinc ions (0.5 mM, 1 mM, and 2 mM) and pH of the reaction mixture (4, 7, and 10); all samples exposed to 50 kGy. UV–vis responses O.D estimated the main influences of parameters on ZnNPs synthesis.

2.4. Characterization analysis

The size and morphology of the synthesized ZnNPs were characterized at National Center for Radiation Research and Technology (NCRRT), Atomic Energy Authority using the following techniques.

2.4.1. UV-VIS spectral analysis

The absorbance of the prepared of ZnNPs was measured by UV spectrophotometer JASCO V-560, Japan in the range from 190 to 800 nm and at a resolution of 1 nm was performed to estimate the Surface Plasmon Resonance (SPR).

2.4.2. Transmission electron microscopy (TEM)

The mean diameter of ZnNPs was investigated using a transmission electron microscopy (TEM), JEOL JSM–100 CX, Japan, with an acceleration voltage of 80 kV. For TEM observations, the samples were prepared by making a suspension from the nanocparticles in acetone using ultrasonic water bath. The suspension was centrifuged to separate the polymer matrix and collimate the large size particles. Then a drop of ZnNPs solution (100 μl) was put into carbon-coated copper grids and the solvent was allowed to evaporate by incubation at 37 °C for 30 min in an incubator.

2.4.3. Dynamic light scattering measurement (DLS)

The size distribution of the prepared ZnNPs nanoparticles was determined using dynamic light scattering (DLS-ZP/Particle Sizer Nicomp 380 ZLS), USA. 250 μl of suspension transferred to a disposable small volume cuvette. After equilibration to a temperature of 25 °C for 2 min, five measurements were performed using 12 runs of 10 s each.

2.4.4. Fourier transform infrared spectroscopy (FTIR)

The chemical structure of samples was investigated by infrared spectrophotometer, JASCO FT-IR 6300, Japan, Spectra were recorded in KBr pellets in th range of 400–4000 cm^{-1}. The spectrum was adjusted at a resolution of 4 cm^{-1}.

2.4.5. X-Ray diffraction (XRD)

X-ray diffraction patterns of ZnNPs were obtained with a XRD-6000 series, Shimadzu Scientific Instruments (SSI), Kyoto, Japan using Ni-filter and Cu-Kα target.

2.5. Nitrate reductase assay

Aqueous extract of fermented fenugreek powder was considered for the assay of nitrate reductase according to the method published previously [33], Aqueous extract of fermented fenugreek powder 2 ml mixed with 2 ml of the assay medium (30 mM KNO_3 and 5% isopropanol in 0.1 M phosphate buffer of pH 7.5). Then, incubated at 25 °C in the dark for 1 h and then 1 ml of 50 mM sulphanilamide and 1 ml of 10 mM NEED (N-(1-naphthyl) ethylenediamine dihydrochloride) solutions were added. The absorbance of the developed color estimated in a UV–vis spectrophotometer at 540 nm.

2.6. Scavenging activity

2,2-diphenyl-1-picrylhydrazyl (DPPH) determined scavenging activity of ZnNPs prepared by natural polysaccarides (CP, Alg, and CS) and biological process (Aqueous extract of fermented fenugreek powder and seed)- picrylhydrazyl (DPPH) radical scavenging; the method of Shimada [34], was used to determine the antioxidant activity. Exactly 4.0 ml ZnNPs was added to a methanol solution of 10 mM DPPH (1.0 ml) on individual tubes. The mixture was rocked and left to stand at room temperature for 30 min. The absorbance of the resulting solution was measured spectrophotometrically at 517 nm. The scavenging activity (%) of DPPH was calculated according to Eq. (1):

$$\text{Scavenging activity}(\%) = [1 - (A_{sample}/A_{control})A_{sample}/A_{control})] \times 100\% \quad (1)$$

2.7. Cytotoxic activity

Ehrlich Ascites Carcinoma Cells (mouse tumor): A line of Ehrlich Ascites Carcinoma (EAC) cells supplied from National Cancer Institute, Cancer Biology Department,egypt, and maintained by weekly I.P. transplantation of 2.5×10^6 cells/mouse.

Cytotoxicity assay: Assay of Cytotoxic activity of ZnNPs synthesized by CP 1%, sodium Alg 1%, CS 1% and aqueous extract of fermented fenugreek powder and determine the 50% inhibition of cell survival (IC_{50}) for the best one; under investigation against Ehrlich Ascites Carcinoma cells. Ascites fluid was withdrawn under aseptic conditions (ultraviolet laminar flow system) from the peritoneal cavity of tumor-bearing mice by needle aspiration after seven days of EAC cell inoculation. Tumor cells obtained was diluted several times with normal saline to adjust the number of EAC cells/ml. EAC viable cells counted by trypan blue exclusion process. Ten μl trypan blue (0.05%) mixed with 10 μl of the cell suspensions. Within 5 min, the mixture spread onto a hemocytometer and a cover slip and then cells examined under a microscope. Dead cells are stained, but viable cells are not [35]. The cells suspension was adjusted to contain 2.5×10^6 viable cells/ml. The cell surviving fraction was calculated according to Eq. (2):

$$\text{Cell surviving fraction} = (T/C) \quad (2)$$

where, T represent the number of viable cells in a unit volume and C is the number of totals (viable + dead) cells in the same unit volume.

The IC_{50} is the concentration of an inhibitor where half diminishes the response. IC_{50}% assay was performed to determine the cytotoxic property of synthesized ZnNPs against EAC and CACO cell lines. A line of human colon adenocarcinoma (CACO) cells obtained from the American Type Culture Collection (ATCC, Rockville, MD). The cells were grown as monolayers in grow on RPMI-1640 medium supplemented with 10% inactivated fetal calf serum and 50ug/ml gentamycin. The cells were sustained at 37 °C in a humidified atmosphere with 5% CO_2 and subcultured two more three times a week. The cells grown as monolayers in growth RPMI-1640 medium supplemented with 10% inactivated fetal calf serum and 50ug/ml gentamycin. The monolayers of 10000 cells adhered at the bottom of the walls in a 96-well Microtiter plate incubated for 24 h at 37 °C in a humidified atmosphere with 5% CO_2. The monolayers washed with sterile phosphate buffer saline (0.01 M pH 7.2) and simultaneously the cell were treated with 100ul from different dilution of the testing sample in fresh maintenance medium and incubated at 37 °C. A control of untreated cells made in the absence of the experiment sample. The positive control, maintaining doxorubicin drug tested as a reference drug for comparison. Use to Six wells for each concentration of the test sample. Every 24 h the investigating the cell under the inverted microscope. The Number of the surviving cells invented by staining of the cells with crystal violet [36,37], followed by cell lysing using 33% glacial acetic acid and read the absorbance at 590 nm using ELISA reader (sunRise, TECAN, Inc, USA) after well mixing. The absorbance values from untreated cell considered as 100% proliferation. Viable cells number deter-

mined using an ELISA reader as previously mentioned before and the viability (%) calculated as according to Eq. (3):

$$\text{Theviability}(\%) = [1 - (OD_t/OD_c] \times 100 \quad (3)$$

Where, OD_t is the mean optical density of wells treated with the tested sample and OD_c are the optical density of the untreated sample. The 50% inhibitory concentration (IC_{50}) The concentration required to cause a toxic effect in 50% of an intact cell, was estimated from graphic plots.

2.8. Antimicrobial activity of ZnNPs

Susceptibility of different bacteria and yeasts to the ZnNPs synthesized by both sodium Alg and aqueous extract of fermented fenugreek powder using Pleurotus ostreatus. An agar well diffusion process [38,39], was use to screen the antibacterial activity. Gram- positive, negative bacteria and yeast *[Bacillus subtilis (RCMB 010067), Staphylococcus aureus (RCMB 010028), Enterococcus faecalis (RCMB 010075), Escherichia coli (RCMB 010052), Pseudomonas aeruginosin (RCMB 010043), Klebsiella pneumonia (RCMB 010093), C.albicans ATCC 10231, C.glabrata ATCC 15126, C.tropicalis ATCC 10610*] Nutrient Agar plates were prepared and swabbed using a sterile L-shaped glass rod with 100 ml of 24 h mature broth culture of individual bacterial strains. The well made by using sterile cork borer 6 mm wells was created into the each Petri plate. Different concentrations of nano-compound (65 μg/ml) were used to assess the activity of the compounds [40].

The material was prepared in sterile water and added to the wells by using sterile micropipettes. Simultaneously the standard antibiotics tetracycline and amphotericin B (as a positive control) were tested against the pathogens. Then the plates incubated at 37 °C for 36 h. After the incubation period, the zone of inhibition of each well measured, and the values were noted. There statistical analysis for antimicrobial activity results performed via SPSS program, version 20(SPSS Inc., Chicago, IL, USA).

3. Results and discussion

3.1. Characterization of ZnNPS synthesized by natural polysaccharides

3.1.1. UV–vis spectroscopy analysis

Fig. 1 shows the UV–vis absorption spectra of ZnNPs synthesized by natural polysaccharides. (CS, Alg and CP). The UV–vis spectroscopic study shows the Plasmon resonance property, confirmed the reduction of zinc ions and formation of ZnNPs with the peak at 375 nm when used Alg and CS; where 300 nm when used CP as reducing and stabilizing agent. The UV Visible absorption spectrum considered as a novel technique used to confirm the presence of ZnNPs. Light white, color observed is due to the Plasmon resonance phenomenon which is the collection of oscillation of electrons. ZnNPs were intensive absorbed in the ultraviolet band of about 300–500 nm [41].

The sharp bands with high intensity of ZnNPs Alg colloids observed at 375 nm, which proves more yield of ZnNPs and size

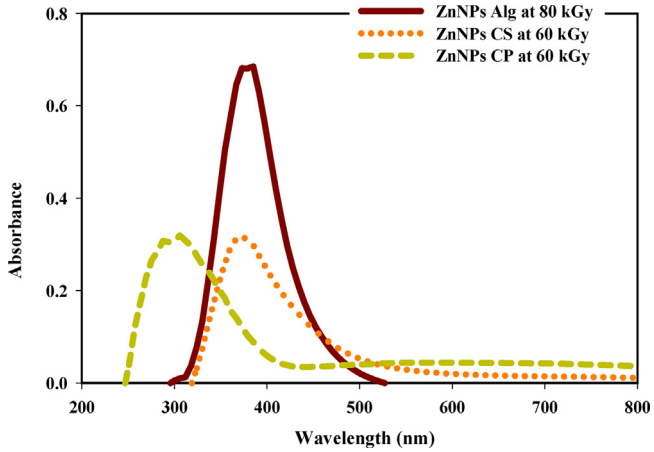

Fig. 1. UV–vis of ZnNPs synthesized by using Alg at 80 kGy, CS at 60 kGy, and CP at 60 kGy.

distribution of the nanoparticles is narrow; sharpness of peak indicated that the particles are monodispersed (Fig. 1). The wavelength and width of the peak depend on the size and distribution of the nanoparticles as well as on the dielectric constant of the metal itself and the surrounding medium [42]. In this study was observed that ZnNPs synthesized by sodium Alg superior to CS and CP.

Table 1 shows the optical density (O.D) of ZnNPs at different λ_{max} depend on types of the polysaccharide. With unirradiated reduction method, ZnNPs not generated where generated in the irradiated process. The advantage of gamma irradiation method for the synthesis of metallic nanoparticles lies in the fact that desired highly reducing radicals without the formation of any byproduct. The radicals and molecules produced in water upon gamma irradiation are e-aq, $OH^{\bullet}$, $H^{\bullet}$, H_2, and H_2O_2. The OH and H radicals are capable to abstract hydrogen from the polymer producing a polymer radical [43–45].

Fig. 1 and Table 1 illustrated that generation of ZnNPs depend on types of natural polysaccharide and dose of radiation. Sodium Alg ZnNPs show high Optical density (0.68) at

80 kGy where CS ZnNPs show optical density (0.32) at 60 kGy, and CP ZnNPs show high optical density (0.31) at 60 kGy. The O.D of ZnNPs synthesized by Alg is greater than CP and CS; this attributed to the formation of a degraded unit of Alg that providing the best growth of ZnNPs with high stability.

The proposed metal ion reduction in solution by ionizing radiation in the presence of a stabilizer. Under the stated experimental conditions the reduction of zinc ions takes place by electron transfer from hydrated electrons and polysaccharide radicals to form zerovalent ZnNPs. We have employed polysaccharide as a reducing agent to Zn^{2+} ions and a stabilizer for ZnNPs. The suggested mechanism for gamma rays were shown according to Eqs. (4)–(9), where RCOH = stabilizing and reducing agent.

$$Zn(NO_3)_2 + H_2O \rightarrow Zn^{2+} + 2NO_3{}^- \quad (4)$$

$$H_2O + \gamma\text{-rays} \rightarrow e^-{}_{aq} + OH^{\cdot} + H^{\cdot} + H_2 + H_2O_2 \quad (5)$$

Table 1
Optical density (O.D) of ZnNPs synthesized by CP, CS and Alg at different irradiation doses.

Radiation doses (kGy)	ZnNPs CS (λ_{max} 375 nm)	Radiation doses (kGy)	ZnNPs CP (λ_{max} 300 nm)	Radiation doses (kGy)	ZnNPs Alg (λ_{max} 375 nm)
Un	0	Un	0	Un	0
10	0.11	10	0.14	10	0.16
20	0.14	20	0.2	20	0.21
40	0.21	40	0.25	40	0.32
60	0.32	60	0.31	60	0.51
80	0.17	80	0.3	80	0.68
100	0.12	100	0.21	100	0.45

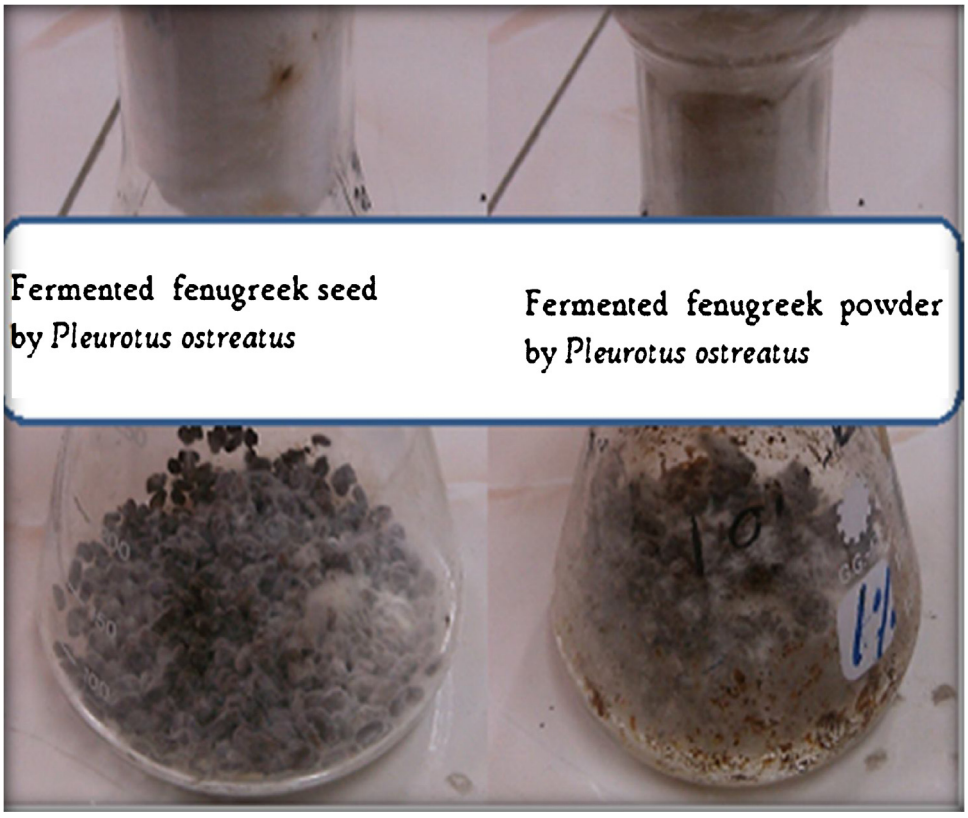

Fig. 2. fermentation of fenugreek seeds and powder by *Pleurotus ostreatus*.

$$Zn^{2+} + 2\,e^{-}_{aq} \rightarrow Zn^{\cdot} \quad (6)$$

$$RC\text{-}OH \rightarrow RC\text{-}O^{\cdot} + H^{\cdot} \quad (7)$$

$$2RC\text{-}O^{\cdot} + Zn^{2+} \rightarrow Zn^{\cdot} + RC\text{-}OH \quad (8)$$

$$nRCO\text{-}OH + Zn^{\cdot} \rightarrow Zn(RC\text{-}OH)n \quad (9)$$

3.1.2. ZnNPs synthesized by fermented fenugreek

The fermentation of fenugreek by *Pleurotus ostreatus* (Fig. 2) and gamma irradiation play a significant role in the biological synthesis of ZnNPs. After mixing of zinc nitrate 1 mM solutionwith aqueous extract of fermented fenugreek (seed and powder) and unfermented (seed and powder) then exposed to gamma ray at 0, 10, 20, 30, 40, 50 and 60 kGy. Aqueous extract of fermented fenugreek powder generates ZnNPs at 50 kGy with big O.D and sharp absorption band at 375 nm (Fig. 3) than other (fermented seed, unfermented powder, and seed). Attributed to the production of byproducts (amino acid, protein, and other fenugreek powder content) that providing the best growth of ZnNPs with high stability. Gamma radiation synergism synthesis of ZnNPs lies in the fact that desired highly reducing radicals can be generated; the reduction of Zn^{2+} ions takes place by electron transfer from hydrated electrons as illustrated in Eqs. (4)–(6).

3.1.3. Experimental factorial design

3.1.3.1. Optical characterization. The collective oscillations of conduction atoms at the surface of nano-sized metal particles

absorb visible electromagnetic waves, this known as Surface Plasmon Resonance (SPR) phenomenon; that estimated the formation of Nanoscale metal particles in the solution medium by simple UV–vis spectrophotometry [46–48]. It is worth mentioning that SPR of metal nanoparticles is greatly a size-dependent phenomenon. The electron scattering augmentation at the surfaces of nanoparticles increase bandwidth and decrease the particle size; hence, variations in bandwidth and shifts in resonance are critical parameters in characterizing the Nano sized regime metal particles. While ZnNPs showed sharp surface Plasmon resonance (SPR) bands at 375 nm confirming the presence of ZnNPs. Higher absorption intensity was due to the formation of more acute phases of ZnNPs. Broadening of the peak indicates the particles are polydispersed.

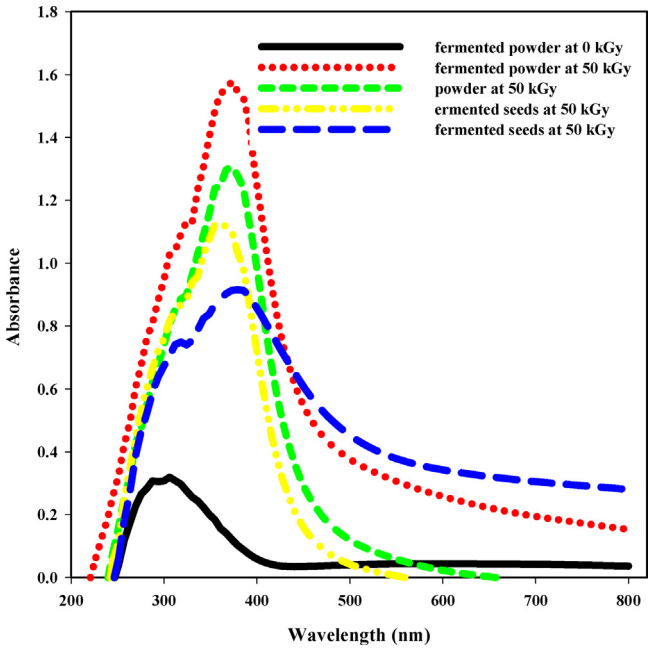

Fig. 3. UV–vis of ZnNPs synthesized by aqueous extract of fermented fenugreek and unfermented (seed and powder) using *Pleurotus ostreatus* and irradiated at 50 kGy.

Table 2
Experimental factorial design temperature effect optical density (O. D) respose.

Run	Factor 1 A: pH	Factor 2 B: Conc.	Factor 3 C: Temp	Response O. D nm
1	10	0.5	60	0.43
2	7	2	100	3.65
3	10	2	100	1.22
4	4	1	60	0.213
5	10	2	60	0.56
6	10	1	100	0.62
7	7	1	100	0.881
8	7	0.5	25	0.15
9	7	1	60	0.521
10	4	2	25	0.21
11	7	2	60	2.83
12	10	1	25	0.31
13	10	1	60	0.61
14	4	0.5	60	0.701
15	4	2	60	0.74
16	7	0.5	60	0.721
17	4	1	100	0.345
18	10	0.5	100	0.154
19	10	2	25	0.281
20	10	0.5	25	0.121
21	4	2	100	1.33
22	4	1	25	0.160
23	4	0.5	25	0.091
24	7	2	25	1.54
25	7	1	25	0.48
26	7	0.5	100	0.876
27	4	0.5	100	0.58

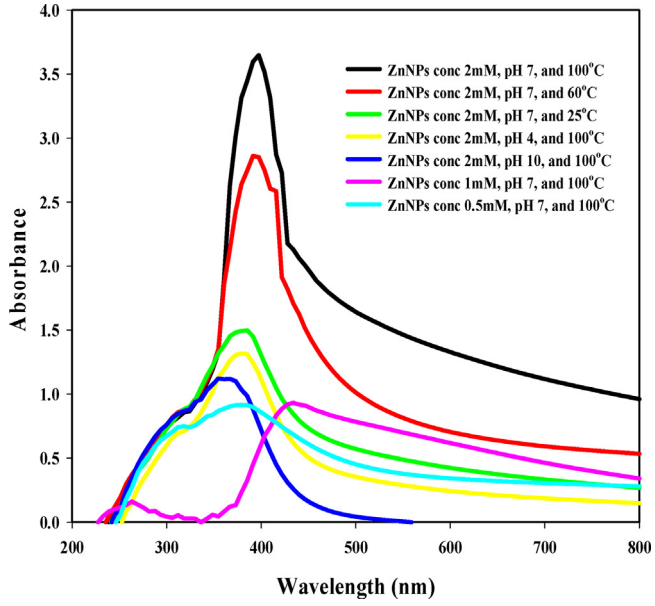

Fig. 4. UV–vis of ZnNPs synthesized by aqueous extract of fermented fenugreek powder using *Pleurotus ostreatus* (highest O.D. experimental factorial design) in case of temperature effect.

3.1.3.2. Effect of temperature. after carrying out 27 experiments in the state of temperature. The results (Table 2), revealed thatrun number 2 (pH7, conc. 2 mM, and 100 °C) give the highest ZnNPs O.D (3.65) at λ_{max} of 396 nm (Fig. 4) than others.

3.1.3.3. Effect of gamma radiation. After carrying out nine experiments in case of 50 kGy, reflecting different combinations of the variables (Table 3), run number 8 (pH 7, conc. 2 mM, 25 °C and 50 kGy) give the highest O. D (4.67) at λ_{max} of 395 nm (Fig. 5) than others in the state of gamma radiation effect.

Figs. 4 and 5 illustrated that peak area and O.D spectrum obtained from the reaction carried out at pH 7 is considerably

Table 3
Experimental factorial design gamma radiation effect optical density (O. D) respose.

Run	Factor 1 A: pH	Factor 2 B: Conc.	Response O.D (50 kGy)
1	4	0.5	0.53
2	4	2	2.90
3	10	0.5	0.61
4	10	1	1.07
5	7	1	1.2
6	4	1	1.40
7	7	0.5	0.81
8	7	2	4.67
9	10	2	1.60

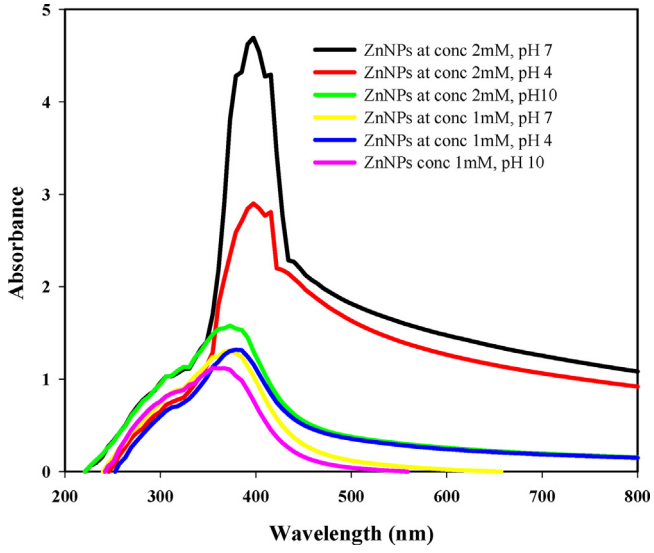

Fig. 5. UV–vis of ZnNPs synthesized by aqueous extract of fermented fenugreek powder using *Pleurotus ostreatus* (highest O. D experimental factorial design) in case of γ-radiation effect (50 kGy).

higher than those obtained at other pHs (4 and 10), indicating its higher

nanoparticle productivity. In this case, variations in the pH of solution have resulted in different arrangements of the capping molecules around the ZnNPs, which affected on the ZnNPs synthesis and the shift in SPR. It knows that the pH of the reaction mixture plays a significant role in synthesis as well as in controlling shape and size of metal nanoparticles [49]. Figs. 4–6 illustrated that radiation most effective than the temperature for synthesis of ZnNPs, lies in the fact that desired highly reducing radicals generated; the reduction of Zn^{2+} ions takes place by electron transfer from hydrated electrons as illustrated in Eqs. (4) and (5).

Fig. 7 illustrated that biological synthesis its superior to natural polysaccharides for production of ZnNPs; ZnNPs synthesized by natural polysaccharides show peak optical density O.D (0.67) at λ_{max} of 375 nm but the aqueous extract of fermented fenugreek using *P. ostreatus* show peak optical density O.D (4.67) at λ_{max} of 395 nm (red shift). The exact position and intensity of the SPR band depend on a variety of factors, including the size and shape of the particles, nature of the solvent and capping agent [50].

3.1.4. Transmission electron microscopy (TEM)

TEM images of ZnNPs synthesized by sodium Alg at the 80 kGy and the aqueous extract of fermented fenugreek powder using Pleurotus ostreatus at 50 kGy Fig. 8a and b respectively. The mean size of ZnNPs Alg 53 nm and the ZnNPs aqueous extract of fermented fenugreek powder 46 nm. Fig. 8a and b illustrated that size of ZnNPs synthesized by the biological method is smallest than that

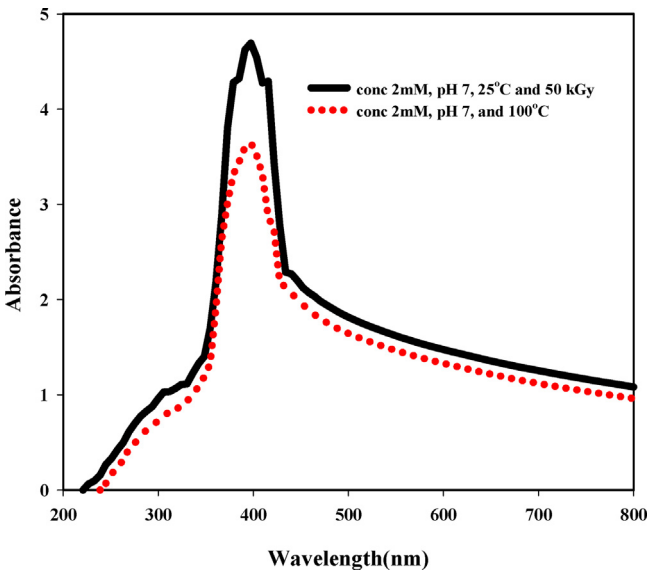

Fig. 6. UV–vis of ZnNPs synthesized by aqueous extract of fermented fenugreek powder using *Pleurotus ostreatus* (highest O.D experimental factorial design) in case of temperature and gamma radiation effect and irradiated at 50 kGy.

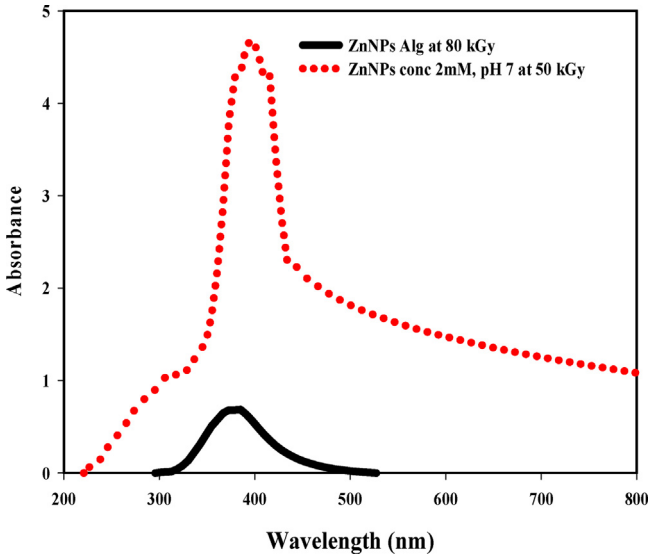

Fig. 7. UV–vis ZnNPs synthesized by aqueous extract of fermented fenugreek powder using *Pleurotus ostreatus* and Alg.

synthesized by natural polysaccharides. Attributed to the presence of byproducts during fermentation (amino acid, protein, enzymes, fibers, polyphenol) that act as reducing agents and capping agents that prevent aggregation and agglomeration of particles.

3.1.5. Dynamic light scattering (DLS)

The particle size and distribution of the synthesized ZnNPs determined using DLS technique. DLS size range of ZnNPs Alg and ZnNPs aqueous extract of fermented fenugreek powder were found to be 89 nm and 84 nm (Fig. 9a and b), respectively. DLS size ranges of ZnNPs was found to be greater than TEM size. Might be because DLS measures the hydrodynamic diameter of nanoparticles, where the amphiphilic nanoparticles were surrounded by water molecules [5,47]; may be attributed to being the cause of the large size of capped formulation.

3.1.6. Fourier transform infrared spectroscopy (FT-IR)

Figs. 10 and 11 shows of ZnNPs Alg and ZnNPs fermented fenugreek, respectively. This analysis was conducted to determine the molecular interaction between the Alg or fermented fenugreek powder and the synthesized ZnNPs. The spectrum in Fig. 11 shows sodium Alg at 0 kGy; an amide C=O transmission at 3340 cm^{-1} assigned to the overlap of O—H and N—H stretching vibrations [51]; 1413 cm^{-1} to C—H bending and 1100 cm^{-1} to —C—O skeletal stretching. The same trend as observed in the sodium Alg at 80 kGy spectrum. For instance, a general decrease or increase in the band with slight shifts; this attributed to degradation of sodium Alg. A

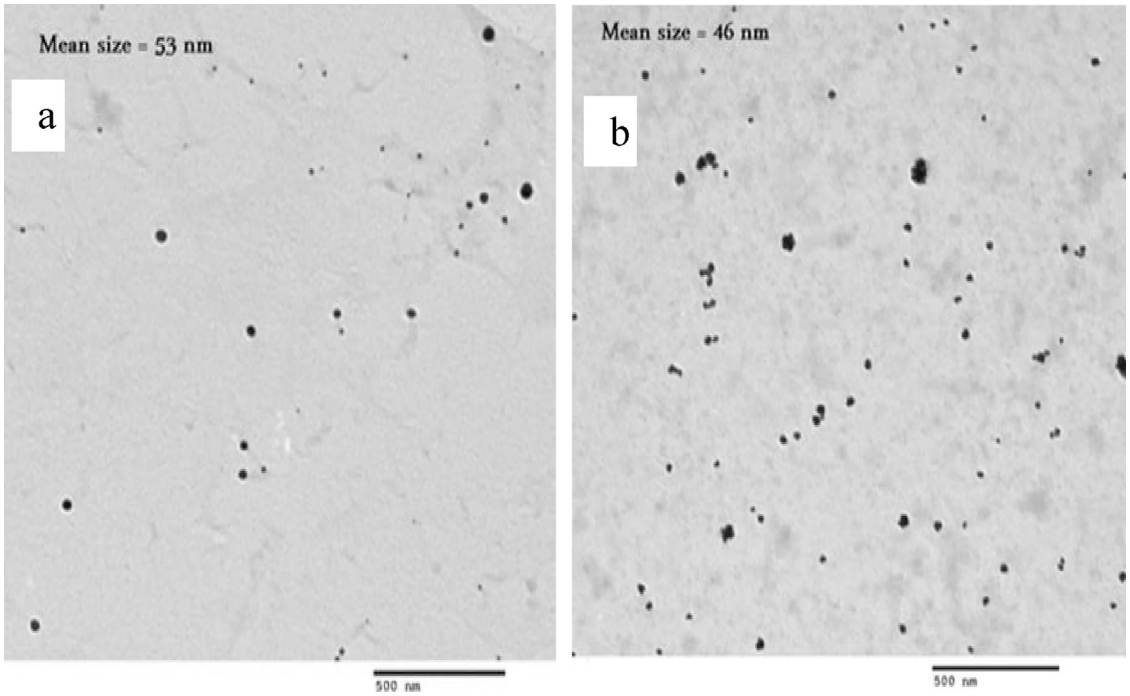

Fig. 8. TEM Micrograph of ZnNPs synthesized by (a) Alg at 80 kGy, and (b) aqueous extract of fermented fenugreek powder using *Pleurotus ostreatus* and irradiated at 50 kGy.

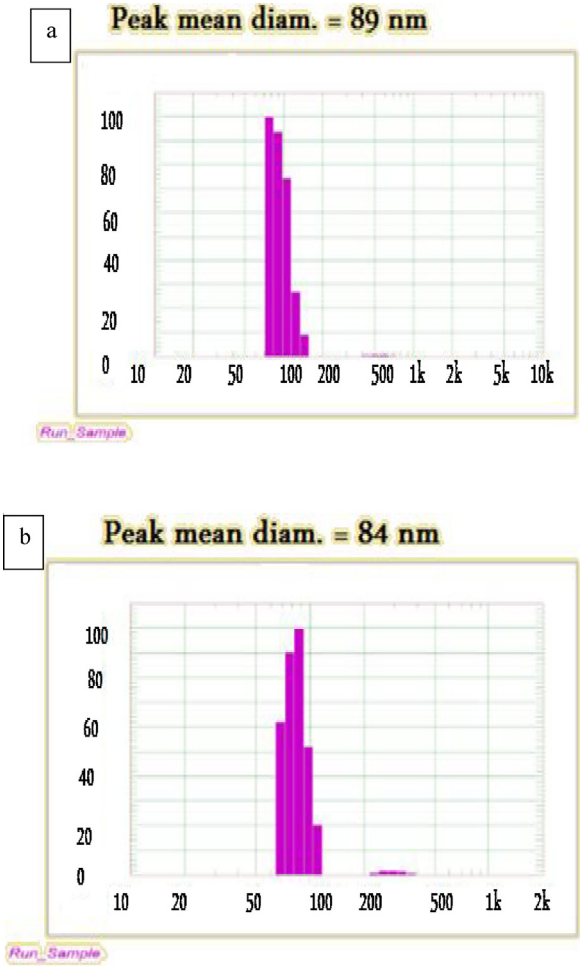

Fig. 9. DLS graph of ZnNPs synthesized by (a) Alg at 80 kGy and (b) aqueous extract of fermented feugreek powder using *Pleurotus ostreatus* and irradiated at 50 kGy.

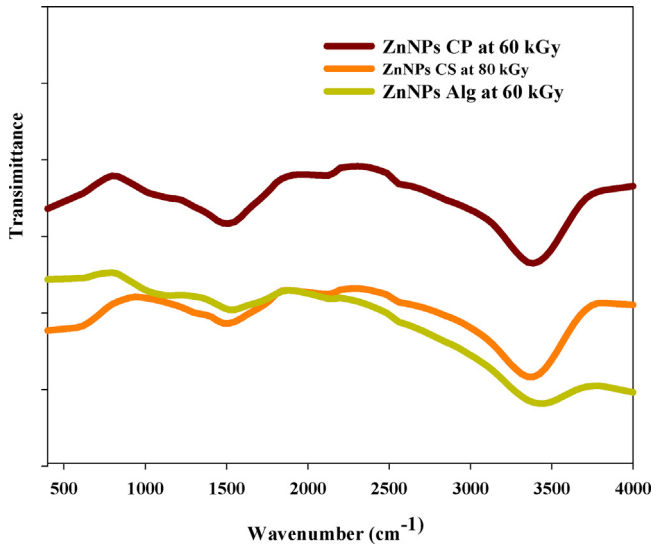

Fig. 10. FTIR spectra of ZnNPs synthesized by CP at 60 kGy, Alg at 80 kGy, CS at 80 kGy.

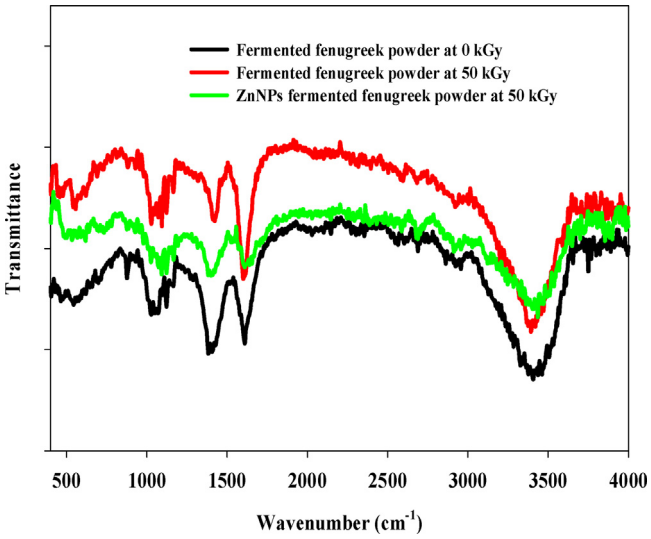

Fig. 11. FTIR spectra of ZnNPs synthesized by aqueous extract of fermented fenugreek powder using *Pleurotus ostreatus* and irradiated at 50 kGy.

similar trend was observed in the ZnNPs spectrum (Fig. 11), which indicates a reaction between the ZnNP surface, and the Alg amino and hydroxyl groups [52].

Fig. 11 shows; fermented fenugreek powder at 0 kGy by *Pleurotus ostreatus* had absorption bands at 3370 cm^{-1}, 2975 cm^{-1}, 1650 cm^{-1}, 1450 cm^{-1}, 1050 cm^{-1}, 777 cm^{-1}; fermented fenugreek powder at 50 kGy by Pleurotus ostreatus had absorption bands at 3375 cm^{-1}, 2985 cm^{-1}, 1660 cm^{-1}, 1440 cm^{-1}, 1070 cm^{-1}, 765 cm^{-1} and ZnNPs fermented fenugreek powder at 50 kGy by Pleurotus ostreatus has absorption bands at 3375 cm^{-1}, 2978 cm^{-1}, 1660 cm^{-1}, 1455 cm^{-1}, 1055 cm^{-1}, 775 cm^{-1}. The broad peak at 3410 cm^{-1} assigned to O—H stretching of hydroxyl group and peak at 2975 cm^{-1} corresponds to asymmetric stretching of C—H bonds. The band at 1650 cm^{-1} assigned to carbonyl and carboxylic (CO) stretching bands of peptide linkages (stretching of amides). The group found at 1450 cm^{-1} can be allocated to —OH bonds of carboxylates. Another band at 1055 cm^{-1} C—N stretching vibrations of primary amines. The ynthesized ZnNPs by fermented fenugreek powder at 50 kGy using *Pleurotus ostreatus* is found to be decreased in the intensity of the peaks that may be due to binding of ZnNPs to —OH groups.

The FT-IR spectrum of ZnNPs by aqueous extract of fermented fenugreek powder at 50 kGy has shown the bands (3415, 1590, 1350, 1380, and 757 cm^{-1}) characteristic of proteins suggesting their role in the stabilization of the nanoparticles. It reported earlier that proteins could bind to nanoparticles either through free amine groups or cysteine residues in the proteins and via the electrostatic attraction of negatively charged carboxylate groups [53], and therefore, stabilization of the ZnNPs of proteins is a possibility.

3.1.7. X-Ray diffraction (XRD)

The end product in the ZnNPs biological and natural polysaccharides synthesis is pale white precipitate after drying on a glass slide at 40 °C. The X-RD. pattern of the ZnNPs synthesized by natural polysaccharides using X-ray diffraction Fig. 12a using sodium Alg shows values at 37.3, 44.2, 65.4, and 77.3 equivalent to (100), (101), (110) and (112) planes in that order. The XRD pattern of the synthesized sample from aqueous extracts of fermented fenugreek powder using *Pleurotus ostreatus* at 50 kGy was recorded on an X-ray diffract meter Fig. 12b. Shows a characteristic peak at 30.1, 34.3, 44.2, 66.1, and 76.3 equivalent to (100), (002),(101) (110) and (112) planes in that order) that are in good agreement with wurtzite

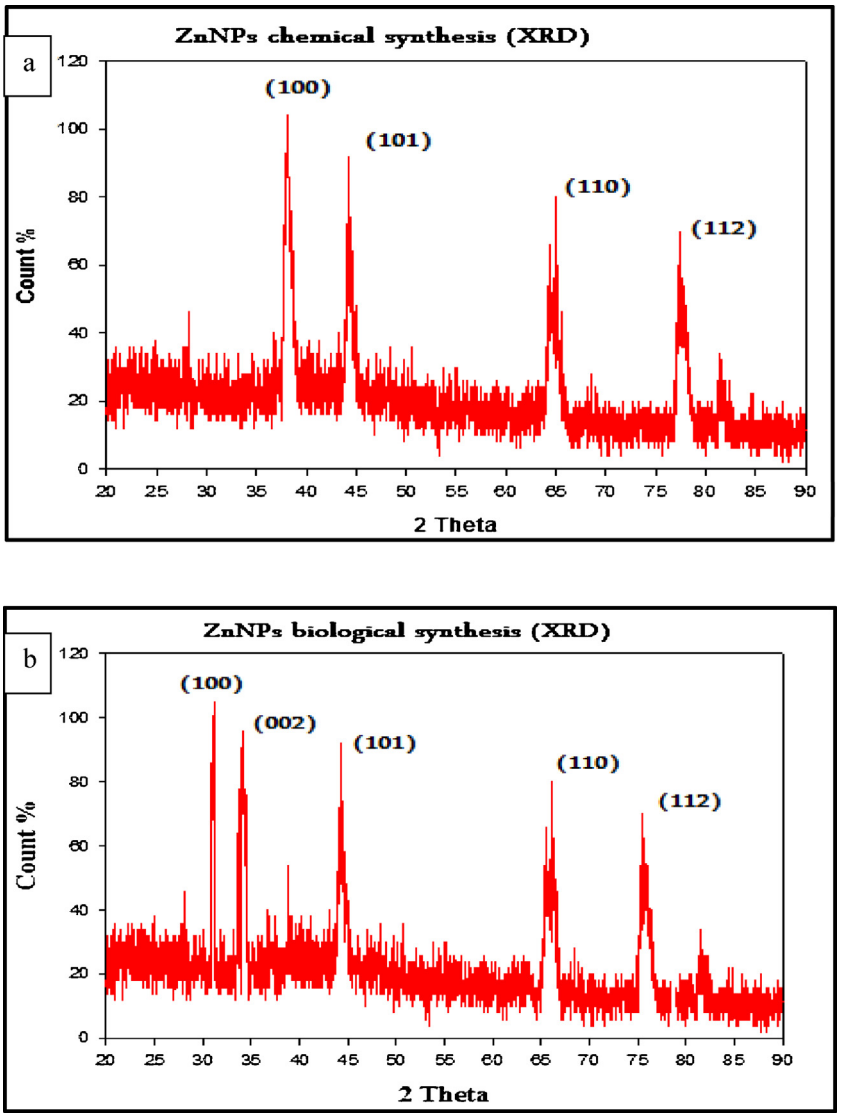

Fig. 12. XRD pattern for the synthesized ZnNPs by (a) Alg at 80 kGy and (b) XRD pattern the ZnNPs synthesized by aqueous extract of fermented fenugreek powder using *Pleurotus ostreatus* and irradiated at 50 kGy.

ZnNPs [54]. The results confirmed that the Zn nanoparticles are of wurtzite hexagonal type structure.

3.2. Nitrate reductase activity

Our study indicated that *Pleurotus ostreatus* didn't secrete extracellular NADH-dependent nitrate reductase enzyme which stated that other reducing factors might be responsible for the nanoparticles synthesis such as proteins, amino acid, and fenugreek powder contents are responsible for the reduction of Zn ions to ZnNPs. Extracellular produced nanoparticles were stabilized by the proteins and reducing agents secreted by the fungus.

The most widely accepted mechanism of silver biosynthesis is the presence of the nitrate reductase enzyme. The enzyme converts nitrate into nitrite. In in vitro synthesis of silver using bacteria, the presence of alpha-nicotinamide adenine dinucleotide phosphate reduced form (NADPH) – dependent nitrate reductase would remove the downstream processing step that is required in other cases. During the reduction, nitrate is converted into nitrite and the electron is transferred to the silver ion; hence, the silver ion is reduced to silver (Ag^+ to Ag^0) [55].

3.3. Scavenging activity (%)

Tables 4 and 5 shows the difference in antioxidant activities before and after ZnNPs synthesis by natural polysaccharides and biological process respectively. The study indicates an increase of antioxidant activities after NPs synthesis; this confirms ZnNPs has antioxidant properties. The antioxidant activities decreased by increase dose of radiation; this attributed to generated free radical during exposed to the solution to gamma rays.

Phenolic and flavonoidal compounds, the biologically active components, are the main agents that can donate hydrogen to free radicals and thus break the chain reaction of lipid oxidation at the first initiation step [56]. This high potential of these compounds to scavenge radicals may be explained by their phenolic hydroxyl groups. It is well known and also reported in the literature that plant mediated nanoparticles synthesis involves sequential reduction followed by capping with these constituents of plants. The results obtained indicated that the antioxidant activity of ZnNPs capped with biological contents or natural polysaccharides possessing free radical scavenging activity

Table 4
Scavenging activity (%) on DPPH.

Radiation dose (kGy)	PC	ZnNPs CP	Radiation dose (kGy)	CS	ZnNPs CS	Radiation dose (kGy)	Alg	ZnNPs Alg
un	60.32	15.12	un	55.02	45.31	un	50.12	48.36
10	45.48	24.45	10	40.23	44.73	10	60.54	62.31
20	30.57	26.72	20	35.34	38.21	20	45.41	48.81
40	20.71	31.18	40	33.54	35.62	40	25.31	31.36
60	10.26	35.39	60	25.32	39.01	60	23.51	28.41
80	8.91	25.27	80	20.21	41.4	80	20.21	30.51
100	5.52	10.63.	100	18.80	40.16	100	18.62	20.51

Table 5
Scavenging activity% of unfermented, fermented fenugreek (seed and powder) and ZnNPs fermented fenugreek powder using DPPH.

Radiation Dose (kGy)	Seed	Fermented seed	Powder	Fermented powder	ZnNPs Fermented powder
0	35.10	40.35	45.12	50.67	60.12
10	25.87	31.67	35.21	40.52	57.41
20	17.12	20.43	25.65	27.90	44.73
30	15.23	18.62	21.83	24.92	40.82
40	13.61	15.72	15.62	20.14	36.52
50	10.51	12.82	11.31	15.63	30.91
60	5.72	10.41	8.42	12.82	26.82

Table 6
Survival cell (%) in Ehrlich ascites carcinoma cell as affected by ZnNPs synthesized CP, Alg, CS and aqueous extract fermented fenugreek powder (AEFFP) using gamma radiation.

R.D (kGy)	CP	ZnNPs CP	Dose (kGy)	CS	Zn NPs CS	Dose (kGy)	Alg	ZnNPs Alg	Dose (kGy)	AEFFP	Zn NPs AEFFP
Un	90.01	88.25	un	90.31	85.31	un	100	95.21	0	10.01	74.67
10	65.14	83.65	10	85.12	81.46	10	100	87.43	10	15.34	68.31
20	70.43	73.65	20	80.70	76.76	20	100	75.76	20	20.03	63.43
40	72.31	68.62	40	95.09	71.92	40	100	64.91	30	23.13	55.72
60	78.42	63.58	60	95.76	67.31	60	100	57.42	40	27.46	51.12
80	82.51	64.79	80	100.0	69.56	80	100	48.01	50	34.03	46.66
100	85.75	69.42	100	100.0	74.32	100	100	51.23	60	41.62	50.25

Table 7
Surviving percent in (EAC) cells as affected by different concentrations of ZnNPs Alg at 80 kGy or by ZnNPs fermented fenugreek powder at 50 kGy after 1 h incubation.

Sample conc. (μg/ml)	Viability% of ZnNPs Alg at 80 kGy	Viability% of ZnNPs fermented fenugreek powder at 50 kGy
65.0000	71.8300	47.0400
32.0000	84.9200	75.1300
16.5000	93.9200	88.7400
8.1250	96.7400	95.5200
4.0625	98.6900	98.7400
2.0315	100.0000	99.3200
0.0000	100.0000	100.0000

Table 8
Surviving percent in (CACO) cells as affected by different concentrations of ZnNPs Alg at 80 kGy and ZnNPs fermented fenugreek powder at 50 kGy after 1 h incubation.

Sample conc. (μg/ml)	Viability% of ZnNPs Alg at 80 kGy	Viability% of ZnNPs fermented fenugreek powder at 50 kGy
65.0000	87.24	71.83
32.0000	95.13	84.92
16.5000	99.72	93.18
8.1250	100	96.74
4.0625	100	98.69
2.0315	100	100
0.0000	100	100

3.4. Cytotoxic activity

The preliminary tumor cytotoxic activities of ZnNPs synthesized by CP, Alg, CS and aqueous extract of fermented fenugreek powder were evaluated against EAC cells at one concentration using trypan blue 0.5% assay. Table 6 summarize the cytotoxicity data of CP, sodium Alg, CS and aqueous extract of fermented fenugreek powder alone and after ZnNPs synthesis against EAC cells after I hour of incubation. The data expressed as the surviving percent. The results showed that EAC cell proliferation significantly inhibited by ZnNPs synthesized by Alg and fermented fenugreek powder at 80 kGy and 50 kGy respectively than others. IC_{50}% assay was performed to determine the cytotoxic property of ZnNPs prepared by Alg and fermented fenugreek powder at 80 kGy and 50 kGy respectively against EAC and CACO cell lines. Treatment of cancer cells with ZnNPs at increasing concentrations (2.0313–65 μg/ml). Table 7 showed cytotoxicity against EAC with 50% inhibition of cell survival (IC_{50}) at a concentration of 60.32 μg/ml (Fig. 13a) and 47.5 μg/ml (Fig. 13b) for ZnNPs Alg and ZnNPs fermented fenugreek powder at 80 kGy and 50 kGy respectively.

The in vitro cytotoxicity of the ZnNPs evaluated against CACO cell line at different concentrations (2.0313–65 μg/ml). Table 8

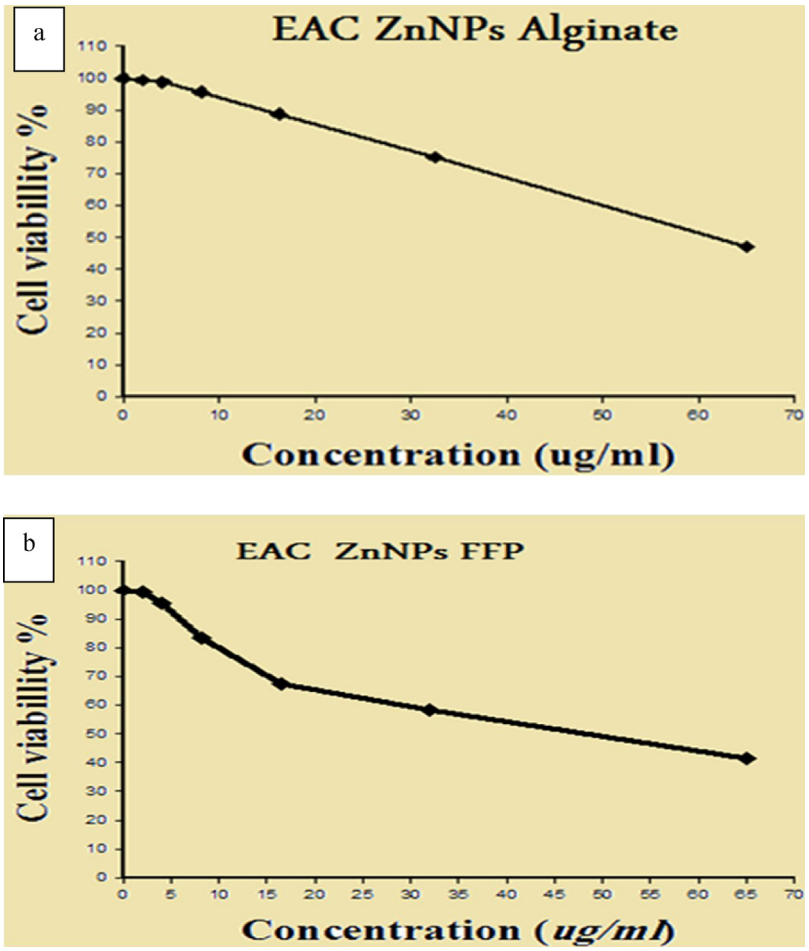

Fig. 13. (a) Cytotoxicity of ZnNPs Alg at 80 kGy against (EAC) cells IC_{50} (60.23 μg/ml and (b) Cytotoxicity of ZnNPs fermented fenugreek powder and irradiated at 50 kGy against (EAC) cells IC_{50} (47.5 μg/ml).

showed the result of surviving percent in (CACO) cells as affected by different concentrations of ZnNPs Alg at 80 kGy and ZnNPs fermented fenugreek powder at 50 kGy after 1 h incubation.

ZnNPs inhibited CACO cells proliferation with the IC50 value >65 μg/ml (Fig. 14a) and (b) for ZnNPs Alg and ZnNPs fermented fenugreek powder at 80 kGy and 50 kGy. In vitro cytotoxicity tests of the ZnNPs Alg and ZnNPs fermented fenugreek on EAC and CACO cell; it observed that ZnNPs more efficient on EAC than CACO cell. Strongly indicated that incorporation of ZnNPs modified the chemical nature of the ZnNPs and caused change the interaction with other molecules such as proteins and others. The cell viability results indicate that ZnNPs are toxic to the EAC and CACO cells.

The cytotoxicity effect of stabilizing and reducing agent (natural polymers and fermented) increased after synthesis of ZnNPs; this growth attributed to the anticancer effect of ZnNPs. The ZnNPs had a cytotoxic effect on tumor cells so they could be used as an antitumorigenic and anticarcinogenic agent [57,58]. A combination of ZnNPs with an anticancer agent (drugs as doxorubicin) reviled that the ZnNPs film deposition on the drug surface led to the selective anticancer activity of composites at the cellular level [59]. ZnNPs have distinct effects on mammalian cell viability via killing cancer while posing no effect on normal cells the marked difference in cytotoxicity between cancer cells and healthy cells suggests an exciting potential for ZzNPs as new alternatives to cancer therapy.

The ZnNPs of size 63 nm and 46 nm are coated with Alg (ZnNPs Alg) and fermented fenugreek powder (ZnNPs FFP) respectively, taken with a series of increasing concentrations (2.031, 4.0625, 8.125, 16.25, 32.5 and 65 μg/ml metal content). In this study, it observed that the synthesized ZnNPs induces a concentration and type of incorporation dependent inhibition of EAC and CACO cells. The ZnNPs FFP showed high cytotoxicity effect compared to ZnNPs; this is mainly due to fermented fenugreek powder has the cytotoxic effect more than Alg so act as the synergistic effect. Moreover, the particle sizes are the difference in ZnNPs FFP (46 nm) than ZnNPs AL (63 nm). Hence in this study, the size-dependent cytotoxicity and stabilizing agents are responsible for Cytotoxicity. Fenugreek extract has a very selective cytotoxicity against cancer cell lines such as T-cell lymphoma (TCP), B-cell lymphomas and breast cancer (MCF7). On the other hand, there no significant cell cytotoxicity amongst normal cells, including human lymphocytes and meningioma, when treated with fenugreek [60]. Apparently, indicates that fenugreek has selective cytotoxic effects against cancer cells.

3.5. Antimicrobial activity

The antimicrobial activity of ZnNPs synthesized by natural polysaccharides (Alg) and biological synthesis (aqueous extract of fermented fenugreek powder using *Pleurotus ostreatus*) tested against pathogenic bacteria and yeasts. The antibacterial properties of the Zn nanoparticles are evaluated against bacterial and fungal strain using the agar well diffusion method. In the agar well diffusion method, the ZnNPs showed significant antibacterial activity on all the bacterial and fungal strains (Table 9). it is clear that the nanoparticles anchor the cell at several sites and cause damage at various locations in the membrane, which could result in cell lysing [61]. If the mechanism of ZnNPs disrupts the outer membrane com-

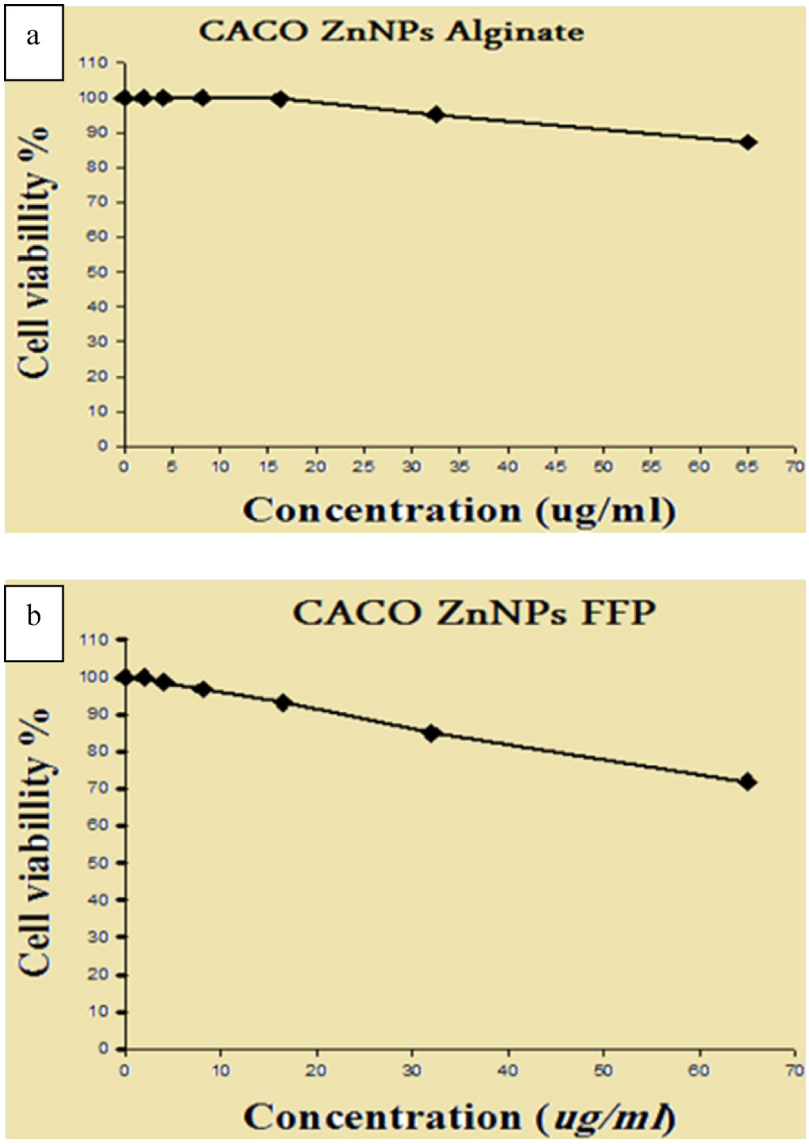

Fig. 14. (a) Cytotoxicity of ZnNPs Alg at 80 kGy against (CACO) cells IC_{50} (>65 μg/ml) and (b) Cytotoxicity of ZnNPs fermented fenugreek powder at 50 kGy against (CACO) cells IC_{50} (>65 μg/ml).

Table 9
The antimicrobial activity (inhibition zone in mm) of ZnNPs synthesized by chemical and biological methods in relation to fermented fenugreek powder and Alg against pathogenic species.

Tested species	Mean diameter of inhibition zone (mm).					
	ZnNPs		Control		Stander	
	ZnNPs Alg	ZnNPs AEFFP	Alg	AEFFP	Tetracycline	Amphotericin B
Bacillus subtilis (RCMB 010067)	15 ± 0.23	20 ± 0.200	6 ± 0.00	8 ± 1.023	18	–
Staphylococcus aureus (RCMB 010028)	9 ± 0.821	12 ± 0.513	6 ± 0.00	7 ± 0.675	29	–
Enterococcus faecalis (RCMB 010075)	14 ± 0.231	16 ± 0.231	6 ± 0.00	7 ± 0.547	23	–
Escherichia coli (RCMB 010052)	19 ± 0.341	22 ± 0.300	6 ± 0.00	9 ± 0.530	28	–
Pseudomonas aeruginosa(RCMB 010043)	15 ± 0.251	17 ± 251	6 ± 0.00	7 ± 1.781	30	––
Klebsiella pneumonia (RCMB 010093)	13 ± 0.230	15 ± 0.235	6 ± 0.00	7 ± 0.916	26	–s
C.albicans ATCC 10231	10 ± 0.115	14 ± 0.115	6 ± 0.00	8 ± 0.371	–	17
C.glabrata ATCC 15126	11 ± 0.263	13 ± 0.173	6 ± 0.00	8 ± 0.419	–	18
C.tropicalis ATCC 10610	10 ± 0.612	12 ± 0.154	6 ± 0.00	9 ± 2.016	–	15

ponents such as poirn and lipopolysaccharide and considering that Gram-positive bacteria do not have an outer layer, then we can conclude the rate of cell destruction should be less severe compared to that of gram-negative bacteria. The antimicrobial efficiency of the Zn nanoparticle depends on the suspension concentration, treatment time, method of synthesis (biological synthesized ZnNPs has activity greater than natural polysaccharides) as well as the strain of microorganism. Based on the results, the ZnNPs has a high potential for decreasing bacteria population so that it may use as an antibac-

terial agent. Also, the results showed that ZnNPs could be a highly effective disinfectant for controlling a broad range of bacteria.

4. Conclusion

In this study, we reported a simple and eco-friendly method for synthesizing ZnNPs using some natural polysaccharides (CS, CP, and Alg) and aqueous extract of fermented fenugreek by *Pleurotus ostreatus* using gamma irradiation, as a novel reducing and stabilizing agent. The synthesized ZnNPs showed superior dispersibility with an average size of 46–53 nm. This approach could be potentially used to industrial large scale synthesis of ZnNPs. The results showed that the synthesized ZnNPs have the antioxidant, cytotoxic and antimicrobial activity due to the smaller size.

Acknowledgment

The authors would like to thank the Nanotechnology Research Unit (P.I. Prof. Dr. Ahmed I. El-Batal), Drug Microbiology Lab., Drug Radiation Research Department, NCRRT, Egypt, for financing and supporting this study under the project “Nutraceuticals and Functional Foods Production by using Nano/ Biotechnological and IrradiationProcesses”.

References

[1] J. Weiss, P. Takhistov, D.J. McClements, Functional materials in food nanotechnology, J. Food Sci. 71 (9) (2006) R107–R116.
[2] F. Danhier, O. Feron, V. Préat, To exploit the tumor microenvironment: passive and active tumor targeting of nanocarriers for anti-cancer drug delivery, J. Controlled Release 148 (2) (2010) 135–146.
[3] R. Bhattacharya, P. Mukherjee, Biological properties of naked metal nanoparticles, Adv. Drug Deliv. Rev. 60 (11) (2008) 1289–1306.
[4] A.M. Elbarbary, N.M. El-Sawy, Radiation synthesis and characterization of polyvinyl alcohol/chitosan/silver nanocomposite membranes: antimicrobial and blood compatibility studies, Polym. Bull. 74 (1) (2017) 195–212.
[5] A.I. El-Batal, G.S. El-Sayyad, A. El-Ghamry, K.M. Agaypi, M.A. Elsayed, M. Gobara, Melanin-gamma rays assistants for bismuth oxide nanoparticles synthesis at room temperature for enhancing antimicrobial, and photocatalytic activity, J. Photochem. Photobiol. B 173 (2017) 120–139.
[6] A.I. El-Batal, K. Azab, H.N. Saada, R.G. Rezk, N.A. El-Tahawy, Ameliorating effect of yeast glucan with zinc bisglycinate in histological and biochemical changes in γ-irradiated rats, Int. J. Agric. Biol. 10 (4) (2008) 361–368.
[7] M.J. Akhtar, M. Ahamed, S. Kumar, M.M. Khan, J. Ahmad, S.A. Alrokayan, Zinc oxide nanoparticles selectively induce apoptosis in human cancer cells through reactive oxygen species, Int. J. Nanomed. 7 (2012) 845–857.
[8] A. Frattini, N. Pellegri, D. Nicastro, O. De Sanctis, Effect of amine groups in the synthesis of Ag nanoparticles using aminosilanes, Mater. Chem. Phys. 94 (1) (2005) 148–152.
[9] P. Vanathi, P. Rajiv, S. Narendhran, S. Rajeshwari, P.K. Rahman, R. Venckatesh, Biosynthesis and characterization of phyto mediated zinc oxide nanoparticles: a green chemistry approach, Mater. Lett. 134 (2014) 13–15.
[10] S. Sinha, I. Pan, P. Chanda, S.K. Sen, Nanoparticles fabrication using ambient biological resources, J. Appl. Biosci. 19 (2009) 1113–1130.
[11] N. Jain, A. Bhargava, J.C. Tarafdar, S.K. Singh, J. Panwar, A biomimetic approach towards synthesis of zinc oxide nanoparticles, Appl. Microbiol. Biotechnol. 97 (2) (2013) 859–869.
[12] S. Ahtzaz, M. Nasir, L. Shahzadi, W. Amir, A. Anjum, R. Arshad, F. Iqbal, A.A. Chaudhry, M. Yar, I. ur Rehman, A study on the effect of zinc oxide and zinc peroxide nanoparticles to enhance angiogenesis-pro-angiogenic grafts for tissue regeneration applications, Mater. Des. 132 (2017) 409–418.
[13] M. Abedini, F. Shariatmadari, M.K. Torshizi, H. Ahmadi, Effects of a dietary supplementation with zinc oxide nanoparticles, compared to zinc oxide and zinc methionine, on performance, egg quality, and zinc status of laying hens, Livestock Science 203 (2017) 30–36.
[14] K.N. Thakkar, S.S. Mhatre, R.Y. Parikh, Biological synthesis of metallic nanoparticles, Nanomed.: Nanotechnol. Biol. Med. 6 (2) (2010) 257–262.
[15] M. Sastry, A. Ahmad, M.I. Khan, R. Kumar, Biosynthesis of metal nanoparticles using fungi and actinomycete, Curr. Sci. 85 (2) (2003) 162–170.
[16] Y. Li, X. Liu, L. Tan, Z. Cui, X. Yang, K. Yeung, H. Pan, S. Wu, Construction of N-halamine labeled silica/zinc oxide hybrid nanoparticles for enhancing antibacterial ability of Ti implants, Mater. Sci. Eng.: C 76 (2017) 50–58.
[17] A. Asokan, T. Ramachandran, R. Ramaswamy, C. Koushik, M. Muthusamy, Preparation and characterization of zinc oxide nanoparticles and a study of the anti-microbial property of cotton fabric treated with the particles, J. Textile Apparel Technol. Manage. 6 (4) (2010) 1–6.
[18] J.E. Jeronsia, L.A. Joseph, M.M. Jaculine, P.A. Vinosha, S.J. Das, Hydrothermal synthesis of zinc stannate nanoparticles for antibacterial applications, J. Taibah Univ. Sci. 10 (4) (2016) 601–606.
[19] A.M. Elbarbary, T.B. Mostafa, Effect of γ-rays on carboxymethyl chitosan for use as antioxidant and preservative coating for peach fruit, Carbohydr. Polym. 104 (2014) 109–117.
[20] H.A.A. El-Rehim, N.M. El-Sawy, E.-S.A. Hegazy, E.-S.A. Soliman, A.M. Elbarbary, Improvement of antioxidant activity of chitosan by chemical treatment and ionizing radiation, Int. J. Biol. Macromol. 50 (2) (2012) 403–413.
[21] Y. Sauvaire, J.C. Baccou, Obtaining Diosgenin,(25R)-spirost-5-ene-3beta-ol; Problems of Acid Hydrolysis of Sapogenins [Trigonella Foenum Graecum, Dioscorea, Tribulus Terrestris]], 1978 [French], Lloydia.
[22] R. Sivaraj, P.K. Rahman, P. Rajiv, S. Narendhran, R. Venckatesh, Biosynthesis and characterization of Acalypha indica mediated copper oxide nanoparticles and evaluation of its antimicrobial and anticancer activity, Spectrochim. Acta Part A: Mol. Biomol. Spectrosc. 129 (2014) 255–258.
[23] P.P. McCue, K. Shetty, A model for the involvement of lignin degradation enzymes in phenolic antioxidant mobilization from whole soybean during solid-state bioprocessing by Lentinus edodes, Process Biochem. 40 (3) (2005) 1143–1150.
[24] A.I. El-Batal, G.S. El-Sayyad, A. El-Ghamery, M. Gobara, Response surface methodology optimization of melanin production by Streptomyces cyaneus and synthesis of copper oxide nanoparticles using gamma radiation, J. Cluster Sci. 28 (3) (2017) 1083–1112.
[25] M. Ghorab, A. El-Batal, A. Hanora, F.M.A. Mosalam, Incorporation of silver nanoparticles with natural polymers using biotechnological and gamma irradiation processes, Br. Biotechnol. J. 16 (1) (2016) 1–25.
[26] M. Kumar, L. Varshney, S. Francis, Radiolytic formation of Ag clusters in aqueous polyvinyl alcohol solution and hydrogel matrix, Radiat. Phys. Chem. 73 (1) (2005) 21–27.
[27] A.F. El-Baz, A.I. El-Batal, F.M. Abomosalam, A.A. Tayel, Y.M. Shetaia, S.T. Yang, Extracellular biosynthesis of anti-Candida silver nanoparticles using Monascus purpureus, J. Basic Microbiol. 56 (5) (2016) 531–540.
[28] A.M. Elbarbary, M.M. Ghobashy, Phosphorylation of chitosan/HEMA interpenetrating polymer network prepared by γ-radiation for metal ions removal from aqueous solutions, Carbohydr. Polym. 162 (2017) 16–27.
[29] N.M. El-Sawy, A. El-Rehim, A. Hassan, A.M. Elbarbary, Radiation grafting of VAc/HEMA binary monomers onto PFA films for biomedical applications, Adv. Polym. Tech. 30 (1) (2011) 21–32.
[30] S.H. Othman, I. Ibrahim, M. Hatab, A.M. Elbarbary, Preparation, characterization and biodistribution in quails of 99 m Tc-folic acid/chitosan nanostructure, Int. J. Biol. Macromol. 92 (2016) 550–560.
[31] A.M. Elbarbary, I. Ibrahim, H. Shafik, S.H. Othman, Magnetic ^{99m}Tc-core-shell of polyethylene glycol/polyhydroxyethyl methacrylate based on Fe_3O_4 nanoparticles: radiation synthesis, characterization and biodistribution study in tumor bearing mice, Adv. Powder Technol. 28 (8) (2017) 1898–1910.
[32] H.A. Abd El-Rehim, D.A. Zahran, N.M. El-Sawy, E.-S.A. Hegazy, A.M. Elbarbary, Gamma irradiated chitosan and its derivatives as antioxidants for minced chicken, Biosci. Biotechnol. Biochem. 79 (6) (2015) 997–1004.
[33] P. Mukherjee, S. Senapati, D. Mandal, A. Ahmad, M.I. Khan, R. Kumar, M. Sastry, Extracellular synthesis of gold nanoparticles by the fungus Fusarium oxysporum, Chembiochem 3 (5) (2002) 461–463.
[34] K. Shimada, K. Fujikawa, K. Yahara, T. Nakamura, Antioxidative properties of xanthan on the autoxidation of soybean oil in cyclodextrin emulsion, J. Agric. Food Chem. 40 (6) (1992) 945–948.
[35] D.A. Ribeiro, M.E.A. Marques, D.M.F. Salvador, In vitro cytotoxic and non-genotoxic effects of gutta-percha solvents on mouse lymphoma cells by single cell gel (comet) assay, Braz. Dent. J. 17 (3) (2006) 228–232.
[36] T. Mosmann, Rapid colorimetric assay for cellular growth and survival: application to proliferation and cytotoxicity assays, J. Immunol. Methods 65 (1–2) (1983) 55–63.
[37] V. Gangadevi, J. Muthumary, Preliminary studies on cytotoxic effect of fungal taxol on cancer cell lines, Afr. J. Biotechnol. 6 (12) (2007) 1382–1386.
[38] C. Perez, M. Pauli, P. Bazerque, An antibiotic assay by the agar well diffusion method, Acta Biologiae et Medicinae Experimentalis 15 (1) (1990) 113–115.
[39] Clinical and Laboratory Standards Institute, Performance Standards for Antimicrobial Susceptibility Testing. Nineteenth Informational Supplement M100-S19, PAClinical and Laboratory Standards Institute, Wayne, 2009.
[40] A. Baraka, S. Dickson, M. Gobara, G.S. El-Sayyad, M. Zorainy, M.I. Awaad, H. Hatem, M.M. Kotb, A. Tawfic, Synthesis of silver nanoparticles using natural pigments extracted from Alfalfa leaves and its use for antimicrobial activity, Chem. Pap. 71 (11) (2017) 2271–2281.
[41] S. Nagarajan, K.A. Kuppusamy, Extracellular synthesis of zinc oxide nanoparticle using seaweeds of gulf of Mannar, *India*, J. Nanobiotechnol. 11 (2013) 39.
[42] J. Gonzalo, R. Serna, J. Solis, D. Babonneau, C. Afonso, Morphological and interaction effects on the surface plasmon resonance of metal nanoparticles, J. Phys.: Condens. Matter 15 (42) (2003) S3001–S3010.
[43] A.I. El-Batal, A.-A.M. Hashem, N.M. Abdelbaky, Gamma radiation mediated green synthesis of gold nanoparticles using fermented soybean-garlic aqueous extract and their antimicrobial activity, SpringerPlus 2 (1) (2013) 129–138.
[44] A. Hanora, M. Ghorab, A.I. El-Batal, F.M.A. Mosalam, Synthesis and characterization of gold nanoparticles and their anticancer activity using gamma radiation, J. Chem. Pharm. Res. 8 (3) (2016) 405–423.

[45] A. El-Batal, B.M. Haroun, A.A. Farrag, A. Baraka, G.S. El-Sayyad, Synthesis of silver nanoparticles and incorporation with certain antibiotic using gamma irradiation, Br. J. Pharm. Res. 4 (11) (2014) 1341–1363.
[46] T.M.D. Dang, T.T.T. Le, E. Fribourg-Blanc, M.C. Dang, The influence of solvents and surfactants on the preparation of copper nanoparticles by a chemical reduction method, Adv. Nat. Sci.: Nanosci. Nanotechnol. 2 (2) (2011) 025004–025010.
[47] A. El-Batal, A. El-Baz, F. Abo Mosalam, A. Tayel, Gamma irradiation induces silver nanoparticles synthesis by Monascus purpureus, J. Chem. Pharm. Res. 5 (8) (2013) 1–15.
[48] A.I. El-Batal, F.A.E.-L. Gharib, S.M. Ghazi, A.Z. Hegazi, A.G.M.A.E. Hafz, Physiological responses of two varieties of common bean (Phaseolus vulgaris L.) to foliar application of silver nanoparticles, Nanomater. Nanotechnol. 6 (2016) 13–28.
[49] Z.L. Wang, Nanostructures of zinc oxide, Mater. Today 7 (6) (2004) 26–33.
[50] R.A. Soomro, S.H. Sherazi, N. Memon, M. Shah, N. Kalwar, K.R. Hallam, A. Shah, Synthesis of air stable copper nanoparticles and their use in catalysis, Adv. Mater. Lett. 5 (4) (2014) 191–198.
[51] P. Chen, L. Song, Y. Liu, Y.-e. Fang, Synthesis of silver nanoparticles by γ-ray irradiation in acetic water solution containing chitosan, Radiat. Phys. Chem. 76 (7) (2007) 1165–1168.
[52] G.T. Cardenas, L. Sanzana, H. Lucia, Synthesis and characterization of chitosan-PHB blends, Boletín de la Sociedad Chilena de Química 47 (4) (2002) 529–535.
[53] L. Rastogi, J. Arunachalam, Sunlight based irradiation strategy for rapid green synthesis of highly stable silver nanoparticles using aqueous garlic (Allium sativum) extract and their antibacterial potential, Mater. Chem. Phys. 129 (1) (2011) 558–563.
[54 Z. Tao, X. Yu, J. Liu, L. Yang, S. Yang, A facile synthesis and photoluminescence of porous S-doped ZnO architectures, J. Alloys Compd. 459 (1) (2008) 395–398.
[55] R. Vaidyanathan, S. Gopalram, K. Kalishwaralal, V. Deepak, S.R.K. Pandian, S. Gurunathan, Enhanced silver nanoparticle synthesis by optimization of nitrate reductase activity, Colloids Surf. B: Biointerfaces 75 (1) (2010) 335–341.
[56] M.M. Khalil, E.H. Ismail, F. El-Magdoub, Biosynthesis of Au nanoparticles using olive leaf extract: 1st nano updates, Arab. J. Chem. 5 (4) (2012) 431–437.
[57] M.F.A. El Fatoh, M.R. Farag, A. Shafika, M.A. Hussein, M. Kamel, G. Salem, Cytotoxic impact of zinc oxide nanoparticles against ehrlich ascites carcinoma cells in mice, Int. J. Pharma Sci. 4 (3) (2014) 560–564.
[58] A.I. El-Batal, A.M. Hashem, N.M. Abdelbaky, Enhancement of some natural antioxidants activity via microbial bioconversion process using gamma irradiation and incorporation into gold nanoparticles, World Appl. Sci. J. 19 (1) (2012) 1–11.
[59] E.R. Arakelova, S.G. Grigoryan, F.G. Arsenyan, N.S. Babayan, R.M. Grigoryan, N.K. Sarkisyan, In vitro and in vivo anticancer activity of nanosize zinc oxide composites of doxorubicin, Int. J. Chem. Mol. Eng. 8 (2014) 33–38.
[60] A. Alsemari, F. Alkhodairy, A. Aldakan, M. Al-Mohanna, E. Bahoush, Z. Shinwari, A. Alaiya, The selective cytotoxic anti-cancer properties and proteomic analysis of Trigonella Foenum-Graecum, BMC Complement. Altern. Med. 14 (1) (2014) 114–122.
[61] E. Hoseinzadeh, M.-Y. Alikhani, M.-R. Samarghandi, M. Shirzad-Siboni, Antimicrobial potential of synthesized zinc oxide nanoparticles against gram positive and gram negative bacteria, Desalin. Water Treat. 52 (25–27) (2014) 4969–4976.